

Dynamic issues in the SE South America storm surge modeling

Paula Etala

Received: 23 June 2008 / Accepted: 24 March 2009 / Published online: 21 April 2009
© Springer Science+Business Media B.V. 2009

Abstract The southeastern coast of South America is located in one of the most cyclogenetic areas in the Southern Hemisphere. Occasionally, those systems may lead to disastrous flooding. Strong and persistent along-shore winds on the shelf may also result in some coastal flooding of smaller magnitude. Nested depth-averaged numerical models are used for the simulation of the storm surge. This study describes the storm surge dynamics in the area and the consequences of different regimes to the storm surge prediction. The large extension and limited depth of the Argentinean Shelf permits a smooth transition of the storm surge to the Río de la Plata and a relatively long forecast horizon for its innermost zone. On the other hand, it is demonstrated that currents in the navigable channels of the Bahía Blanca estuary are the main cause for a strong tide–surge interaction. There, the relative phase between the meteorological forcing and the tide can shift the peak of the storm surge several hours.

Keywords South America · Storm surge · Tide · Numerical model · Tide–surge interaction

1 Introduction

The extensive continental shelf adjacent to the southeastern South America is a determinant cause in the generation of major storm surges on the open coasts and estuaries. It is prone to the action of along-shore and on-shore winds that lead to water level rising mainly on its northern shallow area (Fig. 1, left). The circulation throughout the shelf sea is affected in different ways by tides, winds, fresh water discharges and neighboring western boundary flows. Palma et al. (2004) analyze the barotropic response of the shelf sea to tidal and seasonal wind forcing, in the first part of a comprehensive set of 3-D model studies which provide a broad perspective on the overall influence of those factors. Simionato et al.

P. Etala (✉)
Department of Meteorology, Naval Hydrographic Service, Comodoro Py 2055,
1104 Buenos Aires, Argentina
e-mail: etala@ara.mil.ar; paulaetala@fibertel.com.ar

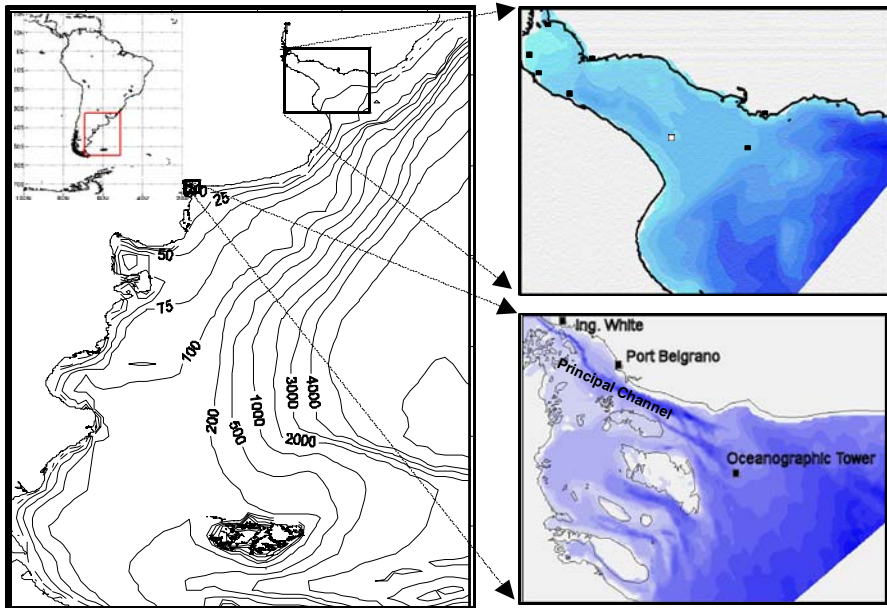


Fig. 1 *Left:* Topography of the SW Atlantic continental shelf (m). *Upper right:* the Río de la Plata model bathymetry and tidal stations; depth ranges from 2 m at the innermost area to 25 m at the mouth. *Bottom right:* model bottom topography and tidal stations in the Bahía Blanca estuary; the maximum depth (*dark blue*) at the Principal Channel is 25 m

(2004) set up a 3-D model for tidal propagation in the shelf sea and two successively nested higher resolution versions for the Río de la Plata area.

The second largest basin in South America discharges to the sea through the Río de la Plata. Its main tributaries, the Paraná and Uruguay rivers, spread through an extensive delta area at its head. The basin is the main waterway of vast and economically active areas of four countries, Argentina, Uruguay, Brazil, and Paraguay, while the region is the most densely populated in Argentina. The two major ports on its shores, Buenos Aires and Montevideo, are also the capital cities of Argentina and Uruguay, respectively. Its main characteristic is its extreme shallowness (Fig. 1, upper right) and extension, that is, a 320-km total length and 230-km width at its mouth. A recent study (Framiñan 2005) proposes its classification into an upper (shallower) estuary, where the circulation is dominated by tides, bottom topography and wind forcing, and a lower section, where interaction with the shelf sea and baroclinic flow are the most relevant features. O'Connor (1991) reproduces the maximum historical storm surges in a domain covering the Río de la Plata and an area of the adjacent shelf, adequate for local southeasterly wind events.

The Bahía Blanca estuary (Fig. 1, bottom right) is an old delta conformation which presents several NW–SE oriented channels separated by large shallow marshes and intertidal flat areas. It is 68-km long and its width is 56 km at the mouth and 200 m at its head. The mean depth is 10 m, with a very irregular bathymetry, up to 25 m in the Principal Channel and large areas <4 m deep. Its upper extreme ends in a 30-km² plain that may be partially flooded. Several important deep water ports provide communication to a very economically active region. This estuary presents particular features in its morphology as well as in its tidal dynamics. The circulation is drastically modified during a tidal

cycle. At high tide, the estuary is almost totally flooded, and only main islands are visible. At low tide, about 900 km² are exposed, only separated by narrow channels. Pierini (2007) presents a depth-averaged model for management purposes, with the strength of an accurate description of topography based on satellite imagery.

1.1 Meteorological background

A characteristic feature of the northern Atlantic coast and the Río de la Plata basin is the presence of upper level troughs associated with frontal systems moving from Southwest to Northeast. These systems interact with the subtropical air masses of the NE of Argentina, N of Uruguay and SW of Brazil, and may lead to cyclogenesis producing strong on-shore winds (i.e., alongshore in the Río de la Plata). The mechanisms that make this region one of the most active areas for cyclone formation in the Southern Hemisphere have been studied by Seluchi (1995). More recently, Mendes et al. (2007) also explain how the Andes plays a major role in controlling the location of the cyclogenesis. Southeasterly winds leading to the most relevant storm surges in the Río de la Plata are produced by two typical synoptic situations that combine a high-pressure system located south and either an associated through or an extra-tropical cyclone centered north, usually over Uruguay. Escobar et al. (2004) find that the former are the most frequent, although the latter lead to the most intense storm surges. The intensity of the winds varies from 20 to 40 km/h for mean events to 70 km/h in the strongest cases (Berri 2001).

It is well known for local oceanographers that southwesterly winds are far from being the only cause to water level rise in the Río de la Plata and the adjacent continental shelf. Strong along-shore winds on the open shelf sea are usually produced in winter by an intense anticyclone over land and deep cyclogenesis over the South Atlantic Ocean moving off the continent. It will be shown here that these systems produce significant and largely extended storm surges along the Atlantic coast and also in the main estuaries, where they are not necessarily related to the local wind.

1.2 Purpose of this study

In most cases, the storm surges are generated on the continental shelf, so they propagate from South to North along the open sea coast as Kelvin waves. The southernmost part of the shelf is known for its large tidal ranges. The magnitude of the tides and tidal currents at the open sea coasts, as well as in the large bays and gulfs, are briefly shown in this article. In some cases, the surge may be extended along the Atlantic coast. Nevertheless, as it has already been mentioned, the shallower northern part of the shelf is the most affected. The damages that the storm surges may produce at the northern Argentinean coast are summarized later in this work. Small-scale coastal features may locally modify currents and water level. This article is not meant to be an exhaustive description of the dynamic of estuaries at the SE South American coast. For such an analysis, the reader is referred to Perillo et al. (1999).

The main interest of this work is to describe the overall mechanisms governing the occurrence of the most relevant storm surges in the southeastern coast of South America, with emphasis on the identification of two different regimes that affect the response to the water level perturbations. Adequate tools have been applied to develop an integral solution to the numerical prediction of the storm surges, including the Río de la Plata and the Bahía Blanca estuary. The resulting numerical forecasting system has been extensively validated and currently, the SMARA numerical storm surge models are producing operational

guidance to contribute to the storm surge prediction. Their performance is systematically monitored with observations along the northern Atlantic coast, the Río de la Plata, and the Bahía Blanca estuary. Complementary results and conclusions on the quality of the guidance produced at its first operational stage in 2007 are presented in Etala (2009). Also, monthly results of the validations are regularly published on-line at <http://www.smn.gov.ar>. This study is mainly based on those models' results. It is focused on the dynamics of the storm surge on the Southwestern Atlantic shelf, where the two main estuaries represent distinguishable behaviors that are relevant to the storm surge prediction.

1.3 Outline

The SMARA set of nested storm surge models is presented in Sects. 2 and 3 describes tides in the estuaries and on the adjacent continental shelf, as well as the model assessment with analyzed data. Section 4 deals with the regional features of the storm surges and their main consequences for society. Storm surges at the Río de la Plata and northern Atlantic coast are the most relevant in the region and so is their human impact. Recent developments in their modeling and prediction are treated separately in Etala (2009). In Sect. 5, the problem of the storm surge modeling in estuaries with strong and complex circulation regimes is addressed from the Bahía Blanca case. The results shown in this section are mainly based on Etala (2000). Finally, results and conclusions are summarized in Sect. 6.

2 The tide and storm surge numerical models

Tides and storm surges in the shelf sea and estuaries are simulated by two-dimensional models, based on the depth-averaged hydrodynamic equations:

$$\frac{\partial h}{\partial t} + \frac{1}{R \cos \Phi} \left[\frac{\partial(Du)}{\partial \Theta} + \frac{\partial(Dv \cos \Phi)}{\partial \Phi} \right] = 0$$

$$\frac{\partial u}{\partial t} + \frac{u}{R \cos \Phi} \frac{\partial u}{\partial \Theta} + \frac{v}{R} \frac{\partial u}{\partial \Phi} - \frac{uv \tan \Phi}{R} - fv = -\frac{g}{R \cos \Phi} \frac{\partial h}{\partial \Theta} - \frac{1}{\rho R \cos \Phi} \frac{\partial p}{\partial \Theta} + \frac{1}{\rho D} (F_s - F_B) + A \nabla^2 u$$

$$\frac{\partial v}{\partial t} + \frac{u}{R \cos \Phi} \frac{\partial v}{\partial \Theta} + \frac{v}{R} \frac{\partial v}{\partial \Phi} + \frac{u^2 \tan \Phi}{R} + fu = -\frac{g}{R} \frac{\partial h}{\partial \Phi} - \frac{1}{\rho R} \frac{\partial p}{\partial \Phi} + \frac{1}{\rho D} (G_s - G_B) + A \nabla^2 v,$$

where (Φ, Θ) are the latitude and longitude, respectively; h is the water elevation above mean sea level (MSL); (u, v) are the depth-averaged current components; $(F_s, G_s) = \vec{T}_S$ is the surface wind stress; $(F_B, G_B) = \vec{T}_B$ is the bottom stress; p is the atmospheric sea level pressure (SLP); $D = \text{MSL} + h$ is the total water depth; ρ is the water density, considered constant; R is the radius of the Earth; g is the acceleration of gravity; A is the horizontal diffusion coefficient; and f , the Coriolis parameter. The quadratic law for bottom stress

$$\vec{T}_B = \rho C_B \vec{q} |\vec{q}|$$

is applied, where \vec{q} is the depth averaged current and $C_B = g/C^2$ is the empirical drag, dependent on the De Chézy coefficient C . Details on the surface wind stress formulation are given in Etala (2009).

The shelf sea is represented at a spatial resolution of $1/3^\circ$ lat. \times $1/3^\circ$ lon. Tidal harmonic constants at the open boundaries are interpolated from global models (Schwidorski 1978a) and subject to calibration to accurately represent tidal constants obtained from tide gauge observations, as shown in the next section. The De Chézy coefficient C is depth (D) dependent for the shelf and constitutes a key model tuning parameter. The final form adopted is

$$C = \begin{cases} 73 & D \leq 50 \text{ m} \\ 93 - \frac{2}{5}D & 50 < D \leq 80 \text{ m} \\ 61 & D > 80 \text{ m} \end{cases}$$

The horizontal diffusion coefficient considered in the shelf model is $A = 5D$ after Glorioso and Flather (1995).

A higher resolution model for the Río de la Plata is nested at $1/20^\circ$ lat. \times $1/20^\circ$ lon. resolution. The tidal constants at the open boundary are interpolated from the Naval Hydrographic Service (SHN) harmonic analyses for two stations located on both shores at the mouth, by following a Kelvin wave shape along the boundary. The storm surge at the open boundaries is provided by the coarse model after the well-known formulation of Davies and Flather (1978). A depth-independent value of 83 is assumed for the De Chézy coefficient, while the horizontal diffusion coefficient is given a constant value of 50.

The circulation in the Bahía Blanca estuary is treated with a similar model which includes a moving boundaries approach, at a very high resolution ($1/180^\circ$ lat. \times $1/120^\circ$ lon.). Tidal constants at the open boundary in this case are interpolated from the shelf model. An oceanographic station located close to the mouth provided the tidal information needed for calibration of the data provided by the coarse model. As in the Río de la Plata, the storm surge values at the open boundaries are obtained from the shelf model. The bathymetry is hydrodynamically defined (Schwidorski 1978b), that is, it considers the realistic inclusion of channels, coastal accidents or islands that may act as barriers to the flux. In this case, the depth-dependent expression for the De Chézy coefficient is

$$C = \begin{cases} 187 & D \leq 1.5 \text{ m} \\ 220 - 22D & 1.5 < D \leq 5 \text{ m} \\ 110 & D > 5 \text{ m} \end{cases}$$

The characteristics of the estuary, as described in the introduction, make it necessary to consider a variable domain and the representation of alternating drying/flooding processes. There are various approaches to this problem, according to local particularities. Here, the algorithm applied to Morecambe Bay by Flather and Heaps (1975), is adopted with slight modifications. The definition of bottom friction in extremely shallow conditions is a major problem in this case. Critical depth is a parameter that represents the threshold for bottom friction to turn independent of depth. A very low critical depth would unrealistically diminish currents close to the drying process, being an obstacle to its completion. On the contrary, a too high critical level would exaggerate currents, particularly at ebb tide, modifying the solution even in deeper areas. In this model, critical depth was set at 2 m. The diffusion coefficient is the same as in the shelf model, with a minimum value of 10. Calibration of the various parameters involved results from a compromise among realistic modeling of tidal range, total drained area at ebb tide and qualitative behavior of currents at limited depth.

3 Discussion of the results of the tidal models

3.1 Tides in the continental shelf sea

The SE South American continental shelf strongly modifies the propagation of the incoming South Atlantic tidal waves. The amphidromes for the main tidal constituents resulting from a numerical model have been first presented in Glorioso and Flather (1995). Here, only M_2 and O_1 cotidal and isoamplitude charts together with tidal current ellipses are shown in Fig. 2. Semidiurnal constituents present two amphidromic systems at the

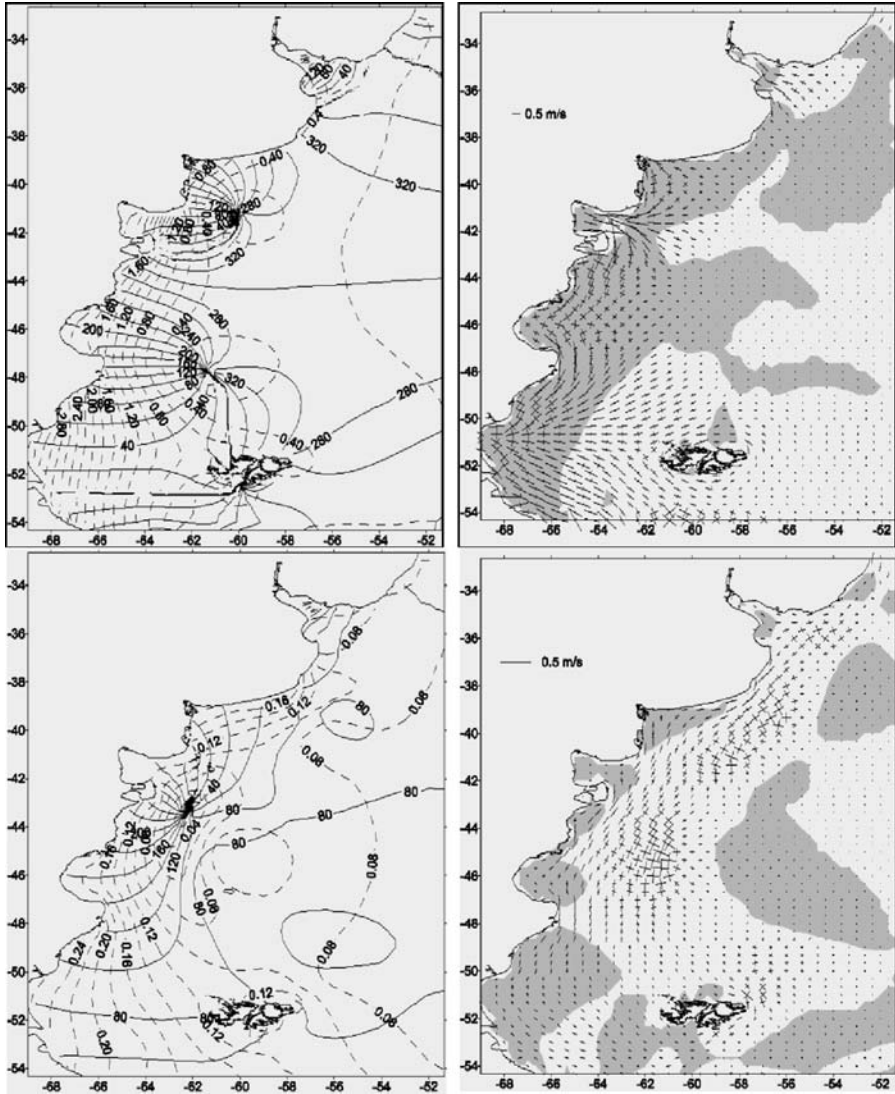


Fig. 2 Left panels: Modeled amplitude (m) and epoch G (°) for the semidiurnal M_2 (upper) and diurnal O_1 (lower) principal lunar tides. Right panels: tidal current ellipses (scale in plot) for the same constituents; currents rotate clockwise in shadowed areas

wider southern shelf while longer diurnal constituents present a single amphidrome strongly dominating tidal propagation. Also considered, but not shown, are the tidal constituents S_2 , N_2 , and K_1 .

Large tidal ranges are found at the southern coasts, as well as in semi-enclosed gulfs. The northern coast adjacent to the Río de la Plata (Fig. 1) is affected by small amplitude tides, while the Bahía Blanca area presents intermediate tidal amplitudes. In Fig. 3, tidal stations on the Atlantic coast are shown. M_2 amplitudes corresponding to the stations in the left panel are plotted in red, from north to south, in the right panel. Blue bars in the same plot correspond to the M_2 amplitudes resulting from the shelf model described in the previous section. The two areas of large tidal amplitudes mentioned above can be clearly noticed. The first zone corresponds to mid-latitude semi-enclosed gulfs. There, it is noted that the shelf model exaggerates amplitudes at the inner station Port Madryn. The most important amplification is found on the open sea coast of the large southernmost bay, where the M_2 amplitudes reach 3.74 m. Amplitudes for islands and off-shore stations (after Glorioso and Flather 1995) are plotted at the end. Tidal current ellipses for all considered constituents have been assessed at three cross-shelf points off-shore Port Madryn, after Rivas (1997), not shown here.

While propagating along the shelf from South to North, an important part of the energy of semidiurnal constituents is dissipated (Glorioso and Simpson 1994) or confined to the two amphidromes present in the wide southern shelf. Bottom friction in the coarse model approach seems unable to balance the shoaling affecting tidal waves as they reach the northern shelf from the deep ocean basin, and some spurious amplification is produced in that area (Fig. 3). The high resolution representation of the adjacent shelf in the Bahía Blanca model, described in the next sub-section, shows a more significant influence of frictional effects. On the other hand, this area seems to keep a subtle balance between gravitational and rotational forces, for the M_2 tide. A high sensitivity was noted in this zone

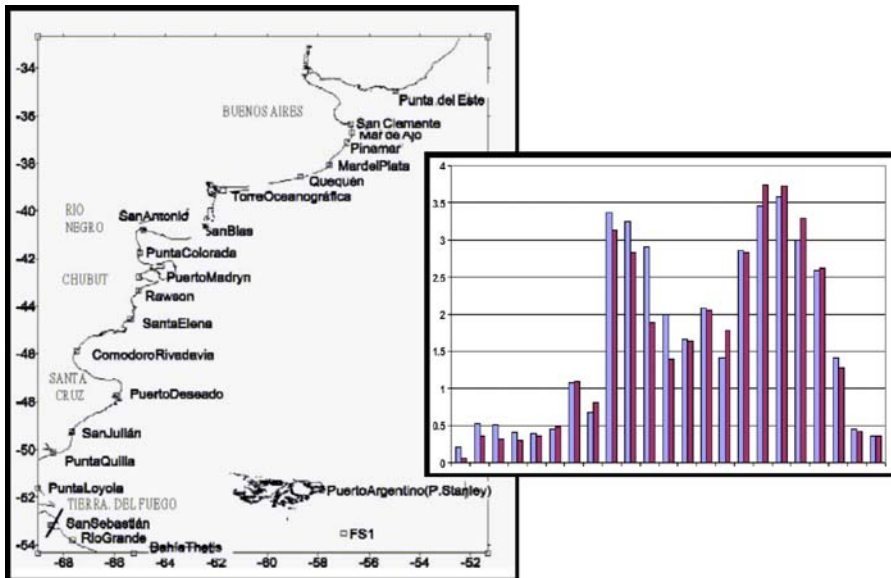


Fig. 3 *Left:* Tidal stations. *Right:* M_2 amplitudes (meters) in left panel stations from north to south, islands last. *Blue:* modeled; *Red:* harmonic analyses. Maximum deviations occur at semi-enclosed gulfs

to an amplification of the southern boundary input needed to accurately represent amplitudes in the south.

3.2 Tides in the Río de la Plata

Tides in the estuaries along the Atlantic coast are forced by the northward propagation of the tidal wave from the shelf. The extremely shallow waters of the Río de la Plata (Fig. 1, upper right) produce wavelengths for semidiurnal tides, so that a wave is almost completely contained from mouth to head. The Río de la Plata is long, converging only at its innermost section and tidal amplitudes are, in general, not amplified toward the head. The tidal regime is mixed, dominantly semidiurnal. The analyzed and modeled collocations of the M_2 principal tide constants for stations in Fig. 1 are shown in Fig. 4. Tidal currents (Framiñan et al. 1999) have been validated in navigation channels for a period of apogee and perigee spring tides against tabulated currents from full spectral analyses based on observations. The model error is within 10% for maximum currents, which are of the order of 1 knot. Instantaneous errors may be larger. Direction bias and standard deviation are both 3° . The time of the slack is in the mean moved 15 min forward. The effect of discharge from tributaries as well as the upstream reach of tides and surges is briefly referred to in the next section.

3.3 Tides in the Bahía Blanca estuary

Observational evidence elsewhere in the literature (Píccolo and Perillo 1990) supports the hypothesis that circulation in the Bahía Blanca estuary (Fig. 1, bottom right) and on the adjacent inner shelf is dominated by the tides and modified by the surge. Moreover, a non-linear interaction between the tide and surge, and the discharge from intertidal areas due to the alternate cycle of flooding and drying processes are dominant features in the circulation of the estuary. A distinctive characteristic of this estuary is that different phases of the tide coexist simultaneously due to the difference in depth among the Principal Channel and the shallow southern channels. The tidal regime is dominantly semidiurnal at the innermost section, due to the amplification of M_2 principal tide. Amplitudes in three stations along the estuary (Fig. 1), i.e., mouth, intermediate, and head, as well as the modeled values are

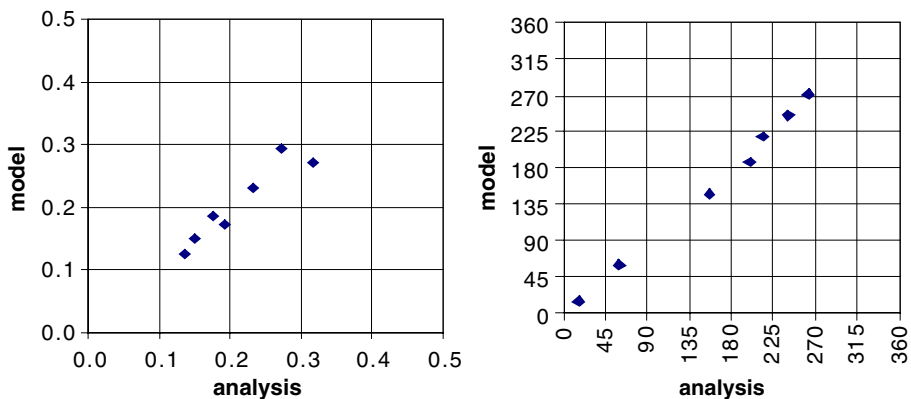


Fig. 4 Collocations of analyzed and modeled M_2 constants at tidal stations in the Río de la Plata. *Left:* amplitudes. *Right:* phases. A wide range of phases is noted

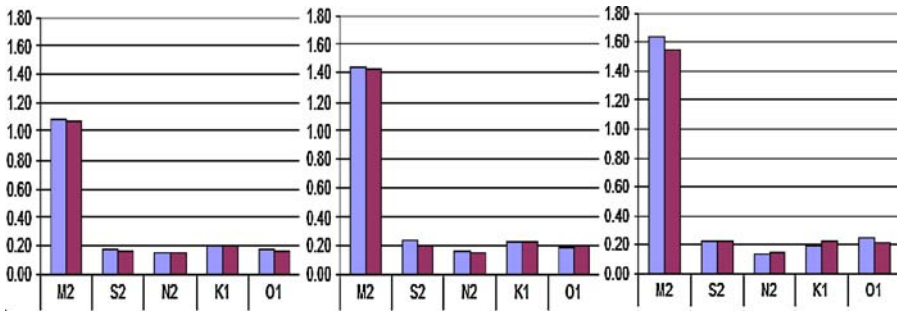


Fig. 5 Amplitudes (m) of the main tidal constituents in the Bahía Blanca estuary. Blue: analyzed, Red: modeled. *Left:* Oceanographic Tower (mouth). *Center:* Port Belgrano (intermediate). *Right:* Ing. White (head). M_2 amplification is noted, while the amplitudes of the other constituents are similar along the estuary

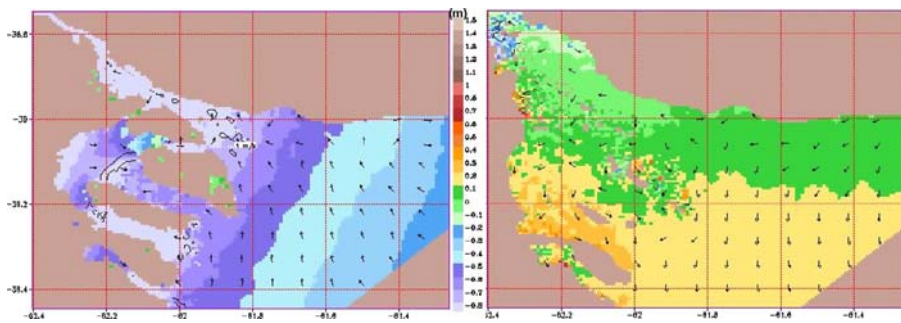


Fig. 6 Surges at ebb (*left*) and flood (*right*) tides in Bahía Blanca. Ebb currents (contour lines for speeds above 1 m/s) constrain to deeper channels as shores and upper estuary flat areas are drained

shown in Fig. 5. Changes in circulation features along the tidal cycle are noticeable, as the estuary may be completely flooded at high tide. Ebb currents intensify, as they are constraint to deeper channels for discharge (Fig. 6, left). Flood currents quickly cover low-lying shores (Fig. 6, right). These results are in agreement with field measurements at the upper Principal Channel from Pícolo and Perillo (1990). It will be shown in Sect. 5 that these processes affect the storm surge in the Principal Channel.

4 Main consequences of the storm surges

4.1 The continental shelf and the shallow northern littoral

Even though the discharge of the Paraná and Uruguay rivers in the Río de la Plata averages 21,000 m³/s (Framiñan et al. 1999), it does not produce any additional elevation of water levels in the Río de la Plata as stated by D’Onofrio et al. (1999) and also suggested by different experiments performed with the SMARA model (not published). Nevertheless, the simultaneous occurrence of extreme flow in the basin, related to El Niño events in the literature (Framiñan 2005), and water level rise in the Río de la Plata, increases the risk of floods in the delta and upstream coasts.

Extreme positive surges due to southeasterly winds can exceed 3 m at the innermost zone of the Río de la Plata. Depending on the concurrence of large-amplitude tides, even

medium intensity surges can lead to floods. According to D’Onofrio et al. (1999), the return period of different evacuation thresholds along the upper Argentinean coast varies from 2.5 to 9 years. Low-lying zones in the city of Buenos Aires and extended areas nearby can be flooded. The usual concurrence of heavy local rain and storms complicates the picture, as the urban and suburban drainage system collapses by the high water level of the Río de la Plata.

The Atlantic coast south of the Río de la Plata is seriously damaged by storm surges and waves during southeasterly storms. Beach material is taken away by the sea, to be then partially transported northward by the long-shore drift (The Argentinean Working Group 1997). The existing dunes constitute a natural defense against the eroding process. Nevertheless, the advance of the cities toward the beach and some coastal structures act against the deposition mechanism and the coastline is prone to erosion. Moreover, the sea violently hits buildings and streets, which have to be evacuated at the occurrence of extreme events.

Figure 7 shows an example of a winter storm surge occurred from July 26 to 28, 2007. Strong along-shore winds on the Argentinean Shelf were produced by a large-scale cyclone, that continued deepening while it moved off-shore. In these cases, the more exposed open coasts of Uruguay are prone to the main damage with the combined effect of ocean waves. A rather large-scale and intense storm surge is produced at almost the complete length of the coast (left panel). It is seen there that also the area of the Bahía Blanca estuary is affected by the water level rise. The storm surge entering the Río de la Plata is shown in the right panel. Due to the shallowness of the continental shelf, the storm surge can be detected at Mar del Plata (Fig. 8, right panel) several hours before it is propagated into the Río de la Plata. This characteristic of the surge dynamics on the shelf permits a relatively long forecast horizon for the inner Río de la Plata, although there is no significant correlation between the local wind and the surge at the estuaries. The observed storm surge at five stations is shown in Fig. 8 (left), as it propagates northward. The

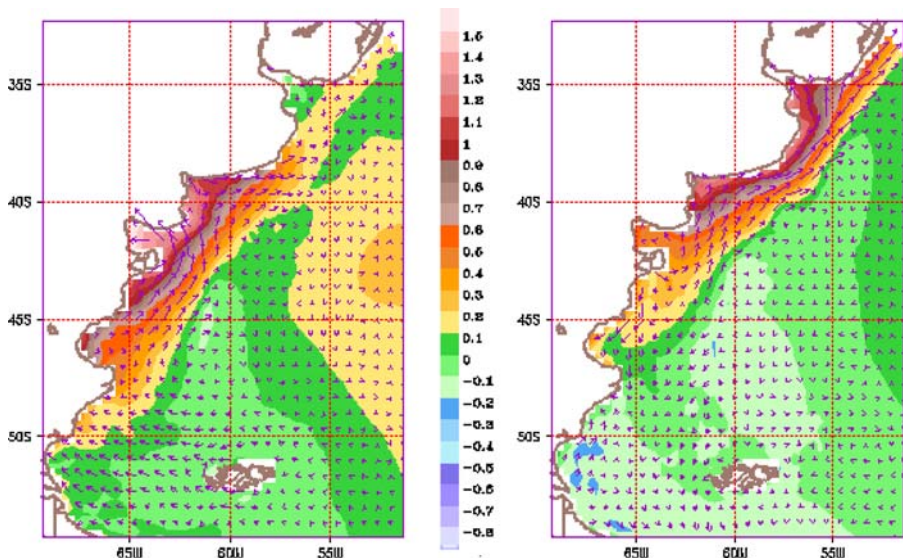


Fig. 7 Two snapshots of a typical winter storm surge due to a deepening large-scale low in SWS Atlantic from July 26 to 28, 2007; the storm surge level is in colors (m) and the total (tide and surge) currents are plotted. The cyclone moves off-shore between 46° S and 42° S (not shown), while the surge extends along the coast, propagating northward

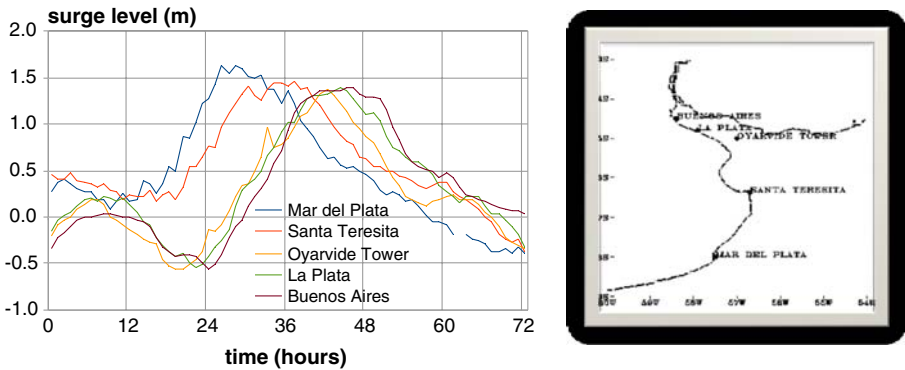


Fig. 8 *Left panel:* The storm surge level (m) at the five stations in the right panel. Time in hours starting at July 26, 2007 00 h local time. La Plata is corrected for bias. *Right panel:* the location of the stations

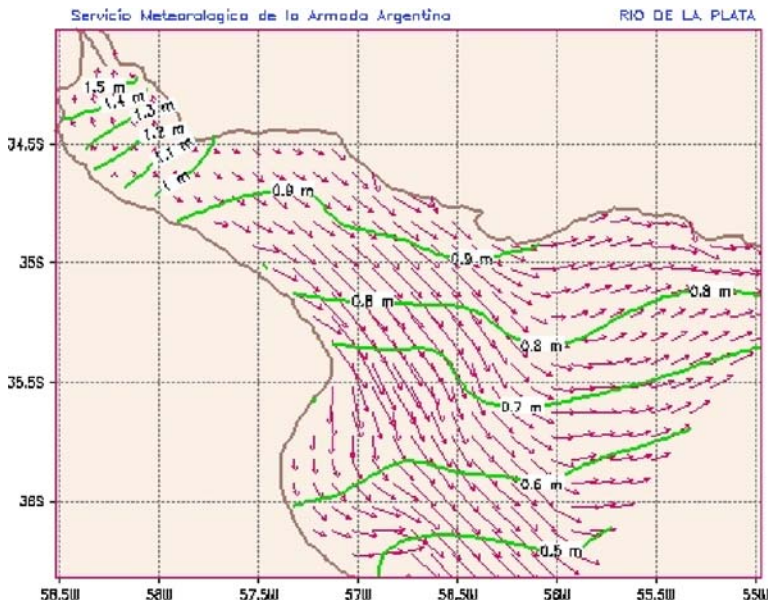


Fig. 9 The storm surge at July 28, 2007 3 h local time produced at the Río de la Plata by the Atlantic coast storm surge in Fig. 7

corresponding modeled values for validation are found in Etala (2009). The amplification or not of the amplitude toward the Río de la Plata depends on the particular wind field distribution and the trajectory of the cyclone. The final set up at the Río de la Plata from the operational hindcast of the SMARA model is seen in Fig. 9. Floods can also happen at its innermost area in these cases, depending on the state of the tide.

4.2 The Bahía Blanca estuary

Storm surges generated along the Bahía Blanca estuary by strong southeasterly winds affect coastal structures, ships and low-lying suburban areas. Even in mild southwesterly

conditions, the contamination produced by untreated sewage is inconveniently displaced upstream. Severe storms are associated with very steep waves, which enhance coastal damage. These storm winds are usually accompanied by heavy rain that also compromises the higher urban zone and terrestrial communications. Intertidal areas are then unexpectedly flooded. The main characteristic of the phenomena is the short notice that the estuary dynamics permit for abnormally rising levels. The length and depth of the estuary cause a short forecast horizon at the head for surge waves that are detected at the oceanographic tower. Apart from that, the extraordinary characteristics of non-linear effects would complicate the prediction of the peak of the storm at the inner estuary, which may occur even before the maximum surge at the mouth, as will be shown in next section.

5 Non-linear surge–tide interactions in a strong tidal regime

The discussion in this section is focused on the non-linear aspects of the storm surge propagation from the shelf into Bahía Blanca and on the important modification it is subject to, due to its highly non-linear behavior. Two different responses to the tide–surge interactions are found throughout the estuary. The well-known phase shift of the tide in the scale of the surge, resulting on the typical oscillations of the surge levels with the period of the tide, is present in the shallower channels and plains. There, limited depth is the main cause of interaction and relative surge maxima occur at rising tide for a positive surge, as expected. The opposite happens in the deeper channels, where relative surge maxima take place at ebb or low tide for a rising surge, due to the dominance of a bottom friction interaction mechanism. The effect of interaction on currents in the channels strongly modifies the water level, and also it changes the normal discharge currents from the intertidal flats. For a better understanding of the combined tide–surge wave response along the Principal Channel, a brief analysis of the bottom friction stress modifications due to the simultaneous influence of tide and surge is presented below.

5.1 Frictional effects

Large tidal ranges and strong currents in the Principal Channel favor the interaction due to the bottom friction modification. Assuming a quadratic dependence of the bottom stress with current, it is clear that in the case of a rising surge, an opposing ebb tidal current of the same order of magnitude would significantly reduce friction, as these counter-currents would tend to compensate. The resulting current is enhanced by the reduced friction, so that in an intense positive surge, a peak is generated at ebb tide. Naturally, the effect would reverse during the decaying stage of the surge, so that the water level modification depends not only on the relative intensity of both tide and surge, but also on their relative phase. Next, the surge–tide interaction is studied in a typical case of southeasterly winds and positive storm surge.

The modeled storm surges at the three locations of Fig. 1 are shown in Fig. 10, left lower panel. The deformation that the surge wave is prone to along the Principal Channel is noted there. It is remarkable that the peak of the storm surge in the inner estuary precedes the peak at the mouth. In order to illustrate the effect of tide–surge interaction, the solution for the surges in the absence of tides is shown in the upper left panel, as compared to the reference solution at Port Belgrano. On the other hand, the observed surge evolution at Port Belgrano is plotted in the right panel for model assessment, together with the total observed water level. From the above reasoning, the enhanced friction in the net flood flux

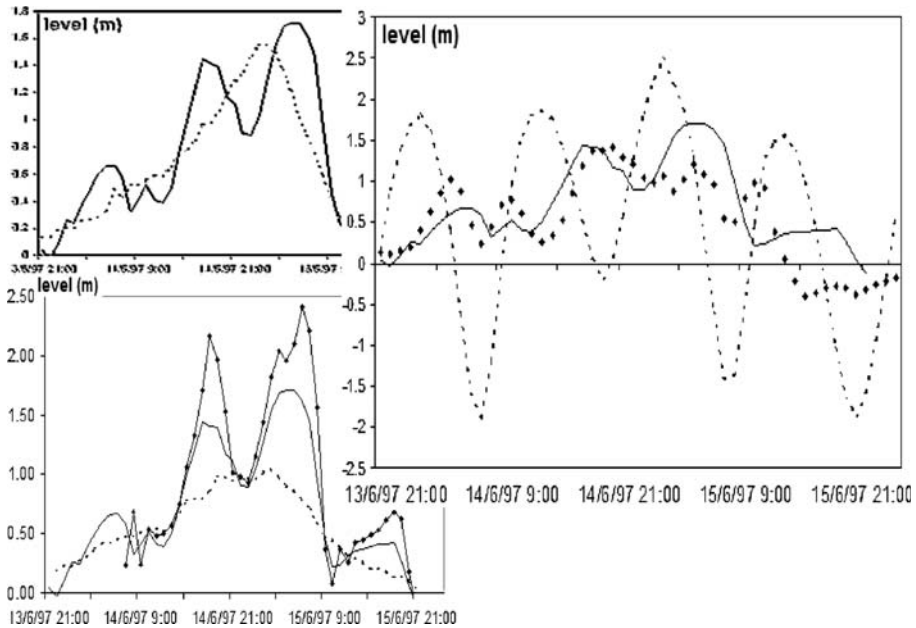


Fig. 10 Water levels during a typical south-easterly storm in Bahía Blanca. *Upper left:* storm surge at Port Belgrano from a no-tide simulation (dashed line) and from the full run (full line). *Lower left:* storm surge at the three locations shown in Fig. 1; dashed: oceanographic tower; full: Port Belgrano; full and dotted: Ing. White. *Right:* total observed water level (dashed), observed (dotted) and modeled (full) surge at Port Belgrano

before the maximum water level, induces the relative depression in the surge. Modeled current intensities during the event are plotted hourly in Fig. 11, together with water level at low and high water (squared dots), to ease the discussion. Ebb currents are shown as positive values and flood currents, as negative. The tidal current cycle (dashed) is separated and the pure surge current (dotted), as isolated from the tidal influence, results negative at the growing stage of the surge and changes sign with the decaying of the storm. The total combined current (full) includes the effect of surge, tide and their interaction, and would correspond to the actual observed current. Finally, the portion of the current due to the effect of interaction (full and dotted), dropping errors, is obtained from

$$F_I = F_{T+S} - F_T - F_S$$

applied to F as (u, v) current components and where suffixes T, S, and I stand for tide, surge, and interaction, respectively.

In this particular case and despite the interaction, the maximum surge would have been reached close to the time of high tide. In Fig. 11, this is inferred from the zero-crossing times of the pure tide and surge current intensities. As opposed to the case analyzed by Proctor and Flather (1989), the maximum surge is moved away from high tide by surge-tide interaction. There, the surge occurred completely around the time of minimum tidal currents, so that the interaction had no time to develop. Here, the surge takes place on a longer time scale than the tide, so that currents interact in the way that is described below.

During the rising stage of the surge (negative surge current) it is clearly seen in Fig. 11 that the total current is increased during the ebb tide, instead of the linear subtraction of

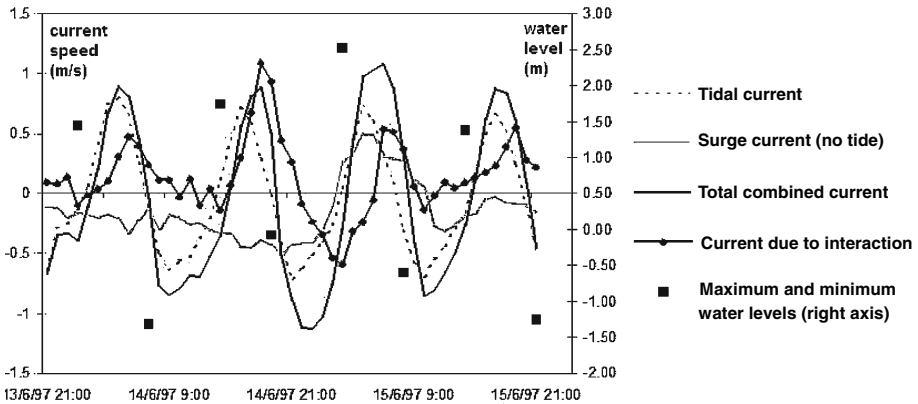


Fig. 11 Modeled currents in Port Belgrano during the southeasterly event of Fig. 10. Ebb currents are shown positive and flood currents, negative. Observed maximum and minimum total water levels are plotted in the secondary axis

currents. The bottom friction is initially diminished due to the opposing currents and an interaction in the direction of the dominant current (ebb) is produced. The maximum interaction is found at the last stage of the ebb, when currents have coexisted for a certain time. The magnitude of this interaction is related to the intensity of the surge, and its maximum value occurs when currents are close in magnitude. This mechanism produces the surge depression that splits the peak into two relative maxima (Fig. 10, upper left). At the time of the maximum tide and storm surge, which in this case approximately coincide, the sudden and simultaneous change in current direction produce a sharp friction decrease, so generating the second surge peak after high tide. According to this analysis, the overall effect of the interaction is a delay of high total water level with respect to the predicted high tide. This result is in agreement with the analysis of water level series in the upper estuary by Perillo and Píccolo (1991).

5.2 Consequences of the interaction for the storm surge prediction

An overestimation of the second peak of the surge is evident when the model results are compared to observations in Fig. 10 (right panel). It will be shown here that, under the conditions described in the previous sub-section, a different relative phase between the meteorological forcing and the tide can shift the surge peak several hours. While the results shown so far have been obtained with a 3-h wind input, the results in Fig. 12 refer to an hourly interpolation of that input. It will be demonstrated that the former cannot provide the accuracy needed in the wind timing. By shifting the wind forcing backward in time, so that the surge starts decaying before the reversing of the tidal currents, the error is practically overcome. The results of two experiments with 1- and 2-h shifts, respectively, are shown in Fig. 12. In the second case, the ebb surge currents acting against flood tide enhance the water level growth before high water. The opposing case is seen with a 2-h delay of the wind forcing ($t+2$), where the exaggeration of the second peak is increased.

On the other hand, different approximations to bottom friction in extreme depth conditions, such as the critical depth parameter (Sect. 2), control the current intensity in very shallow areas, where drying and flooding processes take place. The frictional origin of

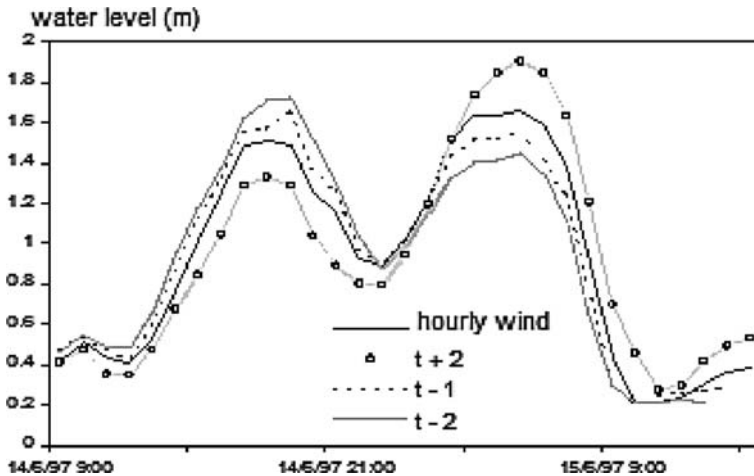


Fig. 12 Total water levels in Port Belgrano as the result of backward (-1 and -2 h) and forward ($+2$ h) shifts in the wind input. The hourly wind is non-shifted and time interpolated. The modulation of the two peaks is highly dependent on wind timing

tide–surge interaction, together with the strong discharge currents, makes those approximations to have a significant impact on the surge, even in the deeper Principal Channel. The importance of considering these effects in the overall calibration process is therefore stressed, to achieve an accurate representation of tide and surge dynamics in these complex regimes.

6 Final remarks

The large SE South America continental shelf provides favorable conditions for the development of storm surges produced by strong and persistent alongshore winds as well as on-shore winds from migratory extra-tropical cyclones. The Río de la Plata, extremely shallow and long, develops the most extreme surges on its highly populated coasts. The transition of the surge wave from the shelf is smooth and relatively slow. The problem of the storm surge modeling with forecasting purposes has been solved by a set of nested models. The definition of the coarse model's domain to account for the surge development along the open sea coast is a determinant factor in the quality of the prediction. Remote forcing can produce significant storm surge events at the open sea coast and in the estuaries.

A highly non-linear regime in a complex topography has been presented. The main interaction mechanism in the deep channel of the Bahía Blanca estuary is bottom friction, while in the shallower areas, it is phase velocity variation. In the scale of the tide, frictional interaction for a growing surge produces surge peaks during ebb tide, while shallow water interaction produces the same effect at rising tide. During this growing stage, the maximum interaction occurs at the ebb tide, as frictional dissipation drastically drops, due to the compensation of currents. With decreasing surge, these effects reverse. The interaction of counter-currents results in the direction of the dominant current. If, on the contrary, tide and surge currents are both in the same direction, the resulting interaction is opposed. This reasoning explains previous field experiment results. Frictional interaction needs high

resolution and realistic currents to be accurately modeled. In every particular case, the characteristics of the interaction depend on a complex balance among dynamic factors which modify the frictional forces, such as the tide and surge ranges, intensity and direction of currents, currents associated to the draining and flooding of shallow areas and flow channeling due to the complex bathymetry, which enhances ebb currents. On the other hand, the relative phase between tide and surge is relevant to the timing and resulting intensity of the storm surge. It was shown that small phase errors can shift 12 h the peak of the surge.

Acknowledgments The models' graphic tools are supported by SM Alonso. Observational data files for validation are maintained by C. Romero. The author is thankful to the anonymous reviewers whose comments contributed to significantly improve this manuscript.

References

- Berri G (2001) Hydrometeorology of floods in Argentina and the Buenos Aires Metropolitan Area (AMBA). In: Kreimer A, Kullock D, Valdés JB (eds) *Floods in the AMBA*. The World Bank Disaster risk management working paper series no. 3. Disaster Management Facility, World Bank, Washington, DC
- D'Onofrio EE, Fiore MME, Romero SI (1999) Return periods of extreme water levels estimated for some vulnerable areas of Buenos Aires. *Cont Shelf Res* 19:1681–1693. doi:[10.1016/S0278-4343\(98\)00115-0](https://doi.org/10.1016/S0278-4343(98)00115-0)
- Davies AM, Flather RA (1978) Application of numerical models of the north west European continental shelf and the North Sea to the computation of the storm surges of November to December, 1973. *Deutsche Hydrographische Zeitschrift, Ergänzungsheft, A*, vol 14, 72 pp
- Escobar G, Vargas W, Bischoff S (2004) Wind tides in the Río de la Plata estuary: meteorological conditions. *Int J Climatol* 24:1159–1169. doi:[10.1002/joc.1026](https://doi.org/10.1002/joc.1026)
- Etala MP (2000) Nested models for the calculation of the storm surge in the Bahía Blanca estuary (in Spanish) PhD thesis. University of Buenos Aires, Buenos Aires
- Etala MP (2009) On the accuracy of atmospheric forcing for extra-tropical storm surge prediction. *Nat Hazards*. doi:[10.1007/s11069-009-9377-0](https://doi.org/10.1007/s11069-009-9377-0)
- Flather RA, Heaps NS (1975) Tidal computations for Morecambe Bay. *Geophys J R Astron Soc* 42:489–517
- Framiñan MB (2005) On the physics, circulation and exchange processes of the Río de la Plata estuary and the adjacent shelf. PhD thesis, University of Miami. Rosenstiel School of Marine and Atmospheric Science, Miami, Florida
- Framiñan MB, Etala MP, Acha EM, Guerrero RA, Lasta CA, Brown OB (1999) Physical characteristics and processes of the Río de la de la Plata estuary. In: Perillo GME, Piccolo MC, Pino-Quivira M (eds) *Estuaries of South America their geomorphology and dynamics*. Springer-Verlag, Berlin, pp 161–194
- Glorioso PD, Flather RA (1995) A barotropic model of the currents off SE South America. *J Geophys Res* 11:1491–1508
- Glorioso PD, Simpson JH (1994) Numerical modelling of the M2 tide on the northern Patagonian Shelf. *Cont Shelf Res* 14:267–278. doi:[10.1016/0278-4343\(94\)90016-7](https://doi.org/10.1016/0278-4343(94)90016-7)
- Mendes D, Souza EP, Trigo IF, Miranda PMA (2007) On precursors of South American cyclogenesis. *Tellus, Ser A, Dyn Meteorol Oceanogr* 59:114–121. doi:[10.1111/j.1600-0870.2006.00215.x](https://doi.org/10.1111/j.1600-0870.2006.00215.x)
- O'Connor WP (1991) A numerical model of tides and storm surges in the Río de la Plata estuary. *Cont Shelf Res* 11:1491–1508. doi:[10.1016/0278-4343\(91\)90023-Y](https://doi.org/10.1016/0278-4343(91)90023-Y)
- Palma ED, Matano RP, Piola AR (2004) A numerical study of the Southwestern Atlantic Shelf circulation: barotropic response to tidal and wind forcing. *J Geophys Res* 109:C08014. doi:[10.1029/2004JC002315](https://doi.org/10.1029/2004JC002315)
- Perillo GME, Piccolo MC (1991) Tidal response in the Bahía Blanca estuary, Argentina. *J Coast Res* 7(2):437–449
- Perillo GME, Piccolo MC, Pino-Quivira M (eds) (1999) *Estuaries of South America their geomorphology and dynamics*. Springer-Verlag, Berlin
- Piccolo MC, Perillo GME (1990) Physical characteristics of the Bahía Blanca estuary. *Estuar Coast Shelf Sci* 31:303–317. doi:[10.1016/0272-7714\(90\)90106-2](https://doi.org/10.1016/0272-7714(90)90106-2)
- Pierini JO (2007) Circulation and transport in the Bahía Blanca estuary coastal zone (in Spanish). PhD thesis, University of Buenos Aires, Buenos Aires
- Proctor R, Flather RA (1989) Storm surge prediction in the Bristol Channel—the floods of 13 December 1981. *Cont Shelf Res* 9:889–918. doi:[10.1016/0278-4343\(89\)90064-2](https://doi.org/10.1016/0278-4343(89)90064-2)

- Rivas AL (1997) Current meter observations in the Argentine continental shelf. *Cont Shelf Res* 17:391–406. doi:[10.1016/S0278-4343\(96\)00039-8](https://doi.org/10.1016/S0278-4343(96)00039-8)
- Schwiderski EW (1978a) Global ocean tides, Part I: a detailed hydrodynamical interpolation model, NSWC/DL TR-3866. Naval Surface Weapons Center, Silver Spring, Maryland
- Schwiderski EW (1978b) Hydrodynamically defined ocean bathymetry, NSWC/DL TR-3888. Naval Surface Weapons Center, Silver Spring, Maryland
- Seluchi ME (1995) Diagnosis and prognosis of synoptic situations leading to cyclogenesis over the east of South America. *Geofis Int* 34:171–186 (in Spanish)
- Simionato CG, Dragani W, Nuñez MN, Engel M (2004) A set of 3-d nested models for tidal propagation from the Argentinean Continental Shelf to the Río de la de la Plata estuary—Part I M2. *J Coast Res* 20(3):893–912. doi:[10.2112/1551-5036\(2004\)20\[893:ASODNM\]2.0.CO;2](https://doi.org/10.2112/1551-5036(2004)20[893:ASODNM]2.0.CO;2)
- The Argentinean Working Group (1997) Evaluation of the Argentinean coast's vulnerability to water level rise (in Spanish). Perillo GME (ed) UNDP–SECYT, Argentina, 62 pp